Proceedings of 20th International Congress on Acoustics, ICA 2010

23-27 August 2010, Sydney, Australia

The correlation between acoustic cavitation and sonoporation involved in ultrasound-mediated DNA transfection with Polyethylenimine (PEI) *in vitro*

Yuanyuan Qiu1 (1), Yi Luo (2), Yanli Zhang (1), Weicheng Cui (1), Dong Zhang (1), Junru Wu (3), Junfeng Zhang (2), Juan Tu (1)

(1) Key Laboratory of Modern Acoustics (Nanjing University), Ministry of Education, Nanjing, Jiangsu, 210093, P. R. China

(2) State Key Lab of Pharmaceutical Biotechnology, School of Life Sciences, Nanjing University, Nanjing 210093, P. R. China

(3) Department of Physics, University of Vermont, Burlington, VT 05405, USA

PACS: 43.10 Df; 43.35 Wa; 43.80 Gx

ABSTRACT

Background: It has been shown that the efficiency of gene/drug delivery can be enhanced under ultrasound (US) exposure with the presence of US contrast agent microbubbles, due to the acoustic cavitation-induced sonoporation. However, obstacles still remain to achieve controllable sonoporation outcome. The general hypotheses guiding present studies were that inertial cavitation (IC) activities accumulated during US exposure could be quantified as IC dose (ICD) based on passive cavitation detection (PCD), and the assessment of sonoporation outcome should be correlated with ICD measurements. **Methods:** In current work, MCF-7 cells mixed with PEI: DNA complex were exposed to 1-MHz US pulses with 20-cycle pulse length and varied acoustic peak negative pressure (P^-; 0 (sham), 0.3, 0.75, 1.4, 2.2 or 3.0 MPa), total treatment time (0, 5, 10, 20, 40 or 60 s), and pulse-repetition-frequency (PRF; 0, 20, 100, 250, 500, or 1000 Hz). Four series experiments were conducted: (1) the IC activities were detected using a PCD system and quantified as ICD; (2) the DNA transfection efficiency was evaluated with flow cytometry; (3) the cell viability was examined by PI dying then measured using flow cytometry; and (4) scan electron microscopy was used to investigate the sonoporation effects on the cell membrane. **Results:** (1) the ICD generated during US-exposure could be affected by US parameters (*e.g.*, P^-, total treatment time, and PRF); (2) the pooled data analyses demonstrated that DNA transfection efficiency initially increased linearly with the increasing ICD, then it tended to saturate instead of trying to achieve a maximum value while the ICD kept going up; and (3) the measured ICD, sonoporation pore size, and cell viability exhibited high correlation among each other. All the results indicated that IC activity should play an important role in the US-mediated DNA transfection through sonoporation, and ICD could be used as an effective tool to monitor and control the US-mediated gene/drug delivery effect.

INTRODUCTION

It has been shown that gene therapy may provide a novel and promising strategy to several presently incurable diseases such as malignant tumor, Parkinson's disease and other genetic diseases [1-3]. One of the most critical tasks is to find a clinically safe and efficient gene delivery method. Although viral vectors can be used as efficient carriers, the strong cytotoxicity and immunogenicity limit their clinical applications [4]. Non-viral vectors are much safer, but the carrying efficiency is relatively low [5]. Polyethylenimine (PEI), one of the most widely used and non-viral gene delivery vector among cationic polymers [6,7], has been shown to be a relatively efficient non-viral agent without additional endosomolytic or lysosomotropic agents [8,9].

Although PEI has shown great success as a non-viral gene delivery vector, it would be more ideal to further increase its transfection efficiency. Many studies have shown that ultrasound (US)-mediated microbubble destruction can enhance DNA transfection efficiency by up to several orders of magnitude both *in vitro* and *in vivo* [10-13]. As reported, US exposure assisted by ultrasound contrast agents (UCAs) could transiently enhance the cell membrane permeability, which could make cell membrane temporarily "open" to facilitate the flux of foreign gene/drugs into cells. This biophysical process is called sonoporation [15-18]. Since US can be non-invasively focused on a target inside the body, US-mediated DNA transfection may achieve *in vivo* gene delivery with high spatial and temporal control, which provides significant clinical advantages [14].

Despite increasing interest in US-mediated gene delivery, the exact mechanism involved in ultrasonic sonoporation process has not fully understood, due to the complexity of US-mediated interactions between cell and microbubbles. It has

been hypothesized that US-induced inertial cavitation (IC) activities (the rapid expansion and violent collapse of gaseous bubbles driven by an US field) should play an important role at sonoporation process [17, 19], and UCA microbubbles added as cavitation nuclei could facilitate the acoustic energy absorption and lower the cavitation threshold [20, 21]. However, obstacles still remain to achieve controllable sonoporation outcome because of the lack of effective exposimetry methods to IC activities. Considering the typical property of IC activities is broad-band noise, in this work we proposed to take real-time measurements of US-induced IC activities with a passive cavitation detection (PCD) system [22], and evaluate the cavitation activities as IC "dose" (ICD) that can reflect the "amount" of IC energy accumulated during a certain US exposure time [23].

The specific hypotheses tested in this work are: (1) IC activities generated during US-mediated DNA transfection should be affected by US parameters, e.g., acoustic peak negative pressure amplitude (P–), pulse-repetition-frequency (PRF) and total treatment time , which could be monitored in real-time and quantified as ICD; (2) With the presence of PEI and UCA microbubbles, the DNA transfection efficiency should be dependent on US parameters and be correlated with the measured ICD; and (3) Sonoporation should be involved in US-mediated DNA transfection, and the size of sonoporation pores on the cell membrane could be highly correlated with ICD measurements. In present work, MCF-7 cells mixed with PEI: DNA complex were exposed to 1-MHz US pulses with varied acoustic parameters. Four series experiments were conducted: (1) The IC activities were detected using a PCD system and quantified as ICD; (2) The DNA transfection efficiency was evaluated with flow cytometry; (3) After dying the cells with PI kit, the viability of the cells was measured using flow cytometry; and (4) The scanning electron microscopy (SEM) was used to investigate the sonoporation effects on the cell membrane..

Current studies would help us to get better understanding on the mechanisms of IC-induced sonoporation and US-mediated DNA transfection with the presence of PEI and UCAs. The long-range goal of this effort is to develop an effective tool to monitor US-induced IC activities in real-time for further optimizing and controlling the sonoporation parameters, and achieving better effect on US-associated gene/drug delivery.

MATERIALS AND METHODS

DNA and other reagents

The plasmid vector pIRES2-EGFP encoding the enhanced green fluorescent protein, was purchased from Clontech (Santa Clara, CA). Branched polyethylenimine with a molecular weight of 25 kDa was purchased from SIGMA-Aldrich (St. Louis, MO, USA). Dulbecco's modified eagles medium (DMEM) was purchased from Invitrogen Corporation (Carlsbad, CA, USA). Fetal bovine serum (FBS) was purchased from GIBCO. PI Detection Kit was purchased from KeyGen Biology Technology Company (Nanjing, China).

Cell lines

Human breast cancer MCF-7 cell line was obtained from American Type Culture Collection (VA, USA). The cells were cultured in DMEM supplemented with 10% FBS and 1% penicillin-streptomycin solution at 37 oC and 5% CO2 atmosphere. The cells were harvested using Trypsin-EDTA (Sigma-Aldrich Co., MO, USA) and resuspended in phosphate buffered saline (PBS; Sigma-Aldrich Co., MO, USA) for the consequent US exposure experiments.

Ultrasound contrast agents

The UCA used here is SonoVue® (Bracco diagnostics Inc., Geneva, Switzerland). It is coated with thin lipid monolayer membrane shell which encapsulates the SF_6 gas, and has a mean radius of ~1.5-3.0 μm. According to the manufacturer's instruction, the purchased SonoVue® vial was vented with a sterile 18-gauge needle, then 5 ml PBS was injected into the vial to have UCA microbubbles reconstituted. The microbubbles were evenly distributed by inversion agitation of the vial which contained 2-5 × 10^8 microbubbles/ml.

Preparation of PEI: DNA complexes

PEI: DNA complexes were prepared by combining 10 μg of plasmid EGFP (pEGFP) in 100 μl PBS with 100 μl PEI (1 mM). The mixture was vortexed for 30 s and incubated at room temperature for 30 min before adding into cell suspension.

Ultrasound exposure and passive cavitation detection system

The US exposure apparatus and PCD system are shown in Fig.1. All experiments were performed in an acrylic tank filled with degassed water. An arbitrary waveform generator (Agilent 33250A, CA, USA) supplied 1-MHz sinusoidal pulses with varied driving amplitude or PRF, and fixed 20-cycle pulse length. The output signals from the waveform generator were amplified through an RF power amplifier (ENI A150, Rochester, NY, USA) with a fixed gain of 50 dB, which were used to drive a 1-MHz self-made focused source transducer with a radius of 9.2 cm, and approximately 6.6-cm focal distance. A plastic test tube of 10-mm diameter and 50-mm length filled with sample suspension (the liquid depth of suspension was ~16 mm) was capped by a rubber stopper that was used as a sound absorber to minimize standing wave effect and then sealed with parafilm to minimize undesired bacteria infection. The test tube was aligned axially with the source transducer so that the center of the suspension was situated at the focal area with respect to the surface of the source transducer.

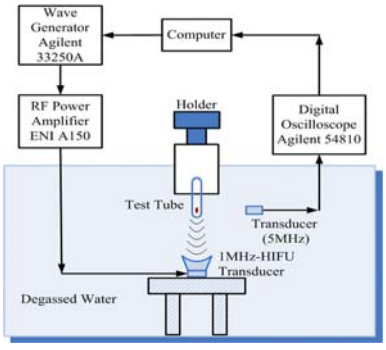

Figure 1. Diagram of US exposure and passive cavitation detection system.

A self-made 5-MHz single-element transducer (11-mm diameter), used for PCD measurements was located perpendicularly to the 1-MHz transducer so that its focus was orthogonal to the source transducer. The bubble scattering and emission signals in the focal volume were collected by the 5-MHz transducer and digitized by an oscilloscope (Agilent 54810, Santa Clara CA, USA). The recorded PCD waveforms were stored in a personal computer (PC) for subse-

quent signal processing using MATLAB program (the MathWorks, Inc., Natick, WA, USA).

Co-focusing of the source and receiver transducers was achieved by using a needle hydrophone (TNU001A, NTR Systems, Inc. Seattle, WA). The movements of needle hydrophone and PCD transducer were conducted *via* 3-D translation stages (Newport Electronics, Inc., Santa Ana, CA, USA). The *in situ* peak negative pressure of the source transducer was calibrated also using the NTR needle hydrophone with a 30-dB preamplifier (HPA30, NTR Systems, Inc. Seattle, WA, USA). The attenuation of the test tube wall was determined by measuring the US amplitude with/without placing the test tube *in situ*.

Transfection protocol using ultrasound

The MCF-7 cells were harvested using Trypsin-EDTA and resuspended in 0.3 ml PBS at a concentration of 2.0×10^6 cells/ml. The PEI:DNA complexes in 0.2 ml PBS and the 1.0×10^7 UCA microbubbles in 0.5 ml PBS were in turn added into the cell suspension individually. Every sample was briefly vortexed before it was exposed to ultrasound.

The influences of acoustic parameters on US-mediated DNA transfection were studies with varied P^-, PRF and total treatment time. In each case, the sample suspension was insonified with a 20-cycle pulse length (the exposure "on" time was 20μs/pulse). The varied ranges for P^-, PRF and total treatment time were 0 to 3.0 MPa, 20 to 1000 Hz, and 5 to 60 s, respectively. Control or "sham" samples were treated in the same way as other samples, but were not exposed to ultrasound. One test was repeated five times for each case.

After US exposure, the cells were centrifuged at 900 rpm for 5 min and collected. For the cell viability assessment, all of the cell pellets were immediately resuspended in PBS and treated with PI dye for the flow cytometry assay. For the SEM investigation, all of the cell pellets were immediately resuspended, and then immobilized, coated and investigated. For the GFP expression assessment, all of the cell pellets were resuspended and cultured in the 6-cell plate, incubated 48 h in DMEM supplemented with 10% FBS and 1% penicillin-streptomycin solution at 37 ^oC and 5% CO_2 atmosphere.

Inertial cavitation dose (ICD) quantification method

Broadband noise emissions produced by IC activities [24] can be detected using a PCD system. Unlike other approaches that only quantify the intensities of IC activities [25, 26], the ICD estimation provides a "dose" measurement to assess the "amount" of IC energy over a certain US exposure duration for different treatment conditions [23].

As shown in Fig.2a, the scattered acoustic signals from the exposed suspension were received by the 5-MHz "listening" PCD transducer and digitized by the oscilloscope with a sampling frequency of 25 MHz. Each waveform of all sampled time series signals (Fig. 2b) was first transformed to the frequency domain using FFT (Fig.2c). A specific frequency window between the second (f_2) and third (f_3) harmonic frequency component (Fig.2c) was chosen to evaluate the amount of IC-induced broadband-noise by calculating the root mean square (RMS) amplitude of the FFT spectrum within the window (Fig.2c). Then these FFT RMS amplitudes were plotted for all sampled waveforms essentially as a function of exposure "on" time (the exposure "on" time = 20 μs/pulse × PRF × treatment time). The cumulated ICD was defined as the area under this curve over the entire exposure "on" time period (*e.g.*, the shadowed area illustrated in Fig. 2d).

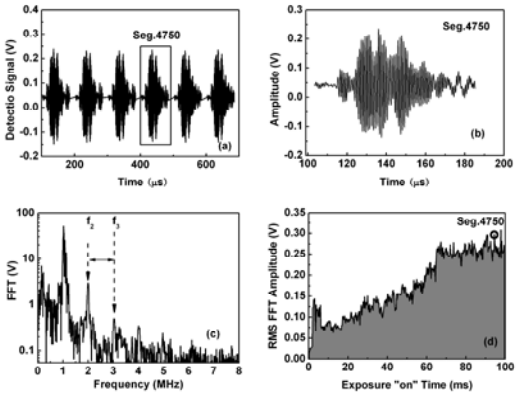

Figure 2. Illustration of ICD computation. For this case, total 5000 signal segments were collected. The detected cavitation signal (a) from each pulse (b) is converted to its frequency spectrum (c). The RMS amplitude within the selected region between f_2 and f_3 in Fig. (c) is calculated for each signal sample and plotted as a function of time in (d). The cumulative RMS FFT amplitudes (integrated gray area in (d)) over the whole exposure "time" gives the ICD.

Assessment of GFP expression

After 48-h incubation in the 6-cell plate, the MCF-7 cells were harvested using Trypsin-EDTA and washed twice in PBS. The collected MCF-7 cell pellets were resuspended at a concentration of approximately 1.0×10^6 cells/ml. The DNA transfection efficiency (referred as the number of cells expressing GFP/number of cells total) was evaluated by assessing the GFP expression of each sample with the flow cytometry (BD FACSCanto™ II, Flowcytometer, Becton Dickinson) at an excitation wavelength of 488 nm.

Assessment of cell viability

The necrotic cells by US exposure are characterized by the broken cell membrane, through which the PI dye could access and stain the nucleus. Such characteristic of PI dye was utilized to tell the necrotic cells from the apoptotic and the normal cells which could prevent from the PI entry by the intact cell membrane. It has been reported that cell membrane damage caused by US exposure can be repaired during a short period [27,28]. Zarnitsyn *et.al.* even theoretically predicted that the IC-induced membrane wounds (~300-nm radius) could be repaired with a half time of 20-50 s [28]. Therefore, in order to avoid PI enter the alive cell through the sonoporation pores, PI dying process was performed 300 s after US exposure to allow the pores getting closed. In detail, the MCF-7 cells were collected by centrifuge at 900 rpm for 5 min and washed twice in PBS. The cells were resuspended, and then immobilized in 70 % ethanol at 4 ^oC overnight. The immobilized cells were collected by centrifuging at 1,200 rpmh for 5 min, resuspended in PBS at a concentration of approximately 1.0×10^6 cells/ml. 5 μl PI solution was added into each cell sample. The mixture was incubated in dark at room temperature for 30 min. After that each sample was analyzed by flow cytometry at an excitation wavelength of 488 nm.

Investigation on cell sonoporation with scanning electron microscopy

To observe US-mediated sonoporation effects on cell membranes, cells for each case were imaged with SEM at 10,000 magnification. After US exposure, the MCF-7 cells were collected by centrifuge and resuspended in PBS, fixed with

2.5% glutaraldehyde solution for 2h at 4°C for 3h, and then washed twice in PBS. Alcohol dehydration was followed in 33%, 50%, 60%, 80%, 90% and 100% ethanol for 20 min respectively. Each step was repeated twice. After been lyophilized using lyophilization (Freezone 6 Freeze Dry System, Labconco Co., Kansas City, Missouri, USA), each sample was gold sputter-coated for 5 min at 125 mA in an argon atmosphere with the approximately 50 nm coating (Emitech K550X Sputter Coating systems, England). A field emission scanning electron microscope (JSM-5610LV, JEOL Ltd., Tokyo, Japan) was used with a gun acceleration voltage of 15 kV and a working distance of 8 mm. The secondary electron was used to image the samples.

Statistic analysis

All data were reported as the mean ± standard deviation (SD) of 5 replicate treatments. One-sided t-test were performed to compare results, with $p<0.05$ considered to be a statically significant difference. Regression analyses were used to determine the correlation between IC dose and the sonoporation outcome. The data were analyzed using Origin software (OriginLab Co., Northampton, MA, USA).

RESULTS

The dependence IC dose on the US parameters

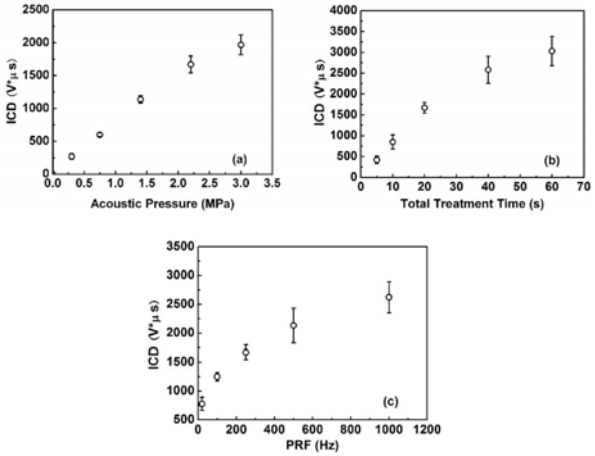

Figure 3. The dependence of ICD on ultrasound parameters. (a) the relationship between ICD and $\bar{P}$, at PRF=250 Hz and treatment time=20 s; (b) the quantified ICD is plotted as a function of treatment time, with $\bar{P}$ = 2.2 MPa, PRF=250 Hz; (c) ICD *vs.* PRF, $\bar{P}$ = 2.2 MPa and treatment time=20 s.

The scattering signals induced by UCA microbubble IC activities were collected as PCD waveforms during the US exposure process. Three series of experiments were carried out to investigate the dependence of the measured ICD on US parameters (*e.g.*, $\bar{P}$, treatment time, or PRF). The sample suspensions mixed with MCF-7 cells, PEI:DNA complexes, and UCA microbubbles were exposed to 1-MHz US at (1) $\bar{P}$ =0 (sham), 0.3, 0.75, 1.4, 2.2, and 3.0 MPa, with fixed PRF of 250 Hz, and total treatment time = 20 s; (2) the total US treatment time varied as: 0 (sham), 5, 10, 20, 40, and 60 s (corresponding to the exposure "on" time of 0, 25, 50, 100, 200, and 300 ms, respectively), with $\bar{P}$ =2.2 MPa, and 250 Hz PRF; and (3) PRF = 0 (sham), 20, 100, 250, 500, and 1000 Hz, at $\bar{P}$ =2.2 MPa, and 20 s treatment time. Fig. 3 illustrates the relationships between ICD and US parameters. As shown in Fig. 3, with other parameters fixed at a constant value, when $\bar{P}$ < 2.2 MPa, treatment time< 20 s or PRF< 250 Hz, ICD almost linearly increases with increased $\bar{P}$, treatment time, or PRF. If we increased the US parameters further, the ICD up-trend gets slow down, and tends saturate eventually, which indicates that the effective IC activities could not be raised unlimitedly by simply enhancing acoustic energy. Since UCAs are suggested to work as cavitation nuclei, the possible explanation for the ICD saturation phenomenon lies in a significant fraction of the available microbubbles is destroyed by strong US pulses, and this issue will be discussed in detail in the Discussion Section.

The influence of ICD on DNA transfection efficiency and cell viability

The influence of ICD on the DNA transfection efficiency and cell viability were investigated here, with varied US parameters. The tested US conditions were also divided into three series as introduced above. In each series, the samples were divided into two groups. For the first group, the DNA transfection efficiencies of all sonicated samples were evaluated by assessing the GFP expression with flow cytometry. The assessments of cell viability were applied to the second group based on PI dying, immediately after US exposure treatment.

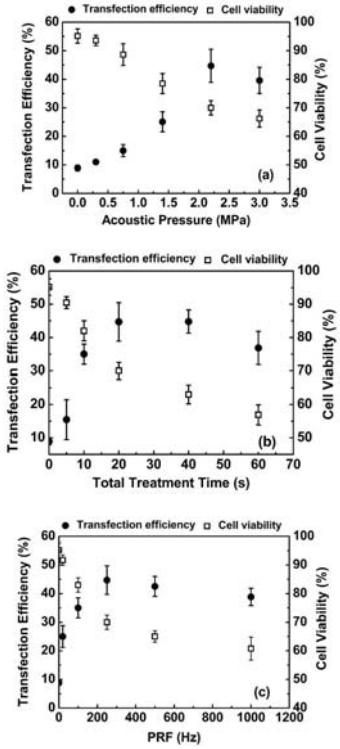

Figure 4. The dependence of DNA transfection efficiency and cell viability on varied US parameters. The reading results of DNA transfection efficiency and cell viability are plotted as a functions of $\bar{P}$ (a), treatment time (b) and PRF (c).

Fig.4a-c illustrates the measured DNA transfection efficiency (*viz*., the reading of GFP fluorescent report) and cell viability as the functions of $\bar{P}$, treatment time and PRF, respectively. As shown in Fig. 4a, the DNA transfection efficiency increases with the increasing of $\bar{P}$ until reaching a peak level of 44.7±5.8% as $\bar{P}$ =2.2 MPa. When $\bar{P}$ >2.2 MPa, the DNA transfection efficiency tends to saturate at a high level around 40%. Meanwhile, the cell viability shows significant decrease with the increasing of $\bar{P}$. The sham group shows the highest cell viability of 95.2±2.5%. The lowest cell viability (66.2±3%) occurs at $\bar{P}$ = 3.0 MPa. Fig. 4b shows, when the total treatment time increases from 0 to 20s, the DNA transfection efficiency increases significantly from 8.9±1% to 44.7±5.8%. If the treatment time increases further, the DNA

transfection efficiency saturates, even tends to decrease slightly with 60-s US treatment. The cell viability keeps decreasing from 95.2±2.5% to 56.9±3%, when the treatment time changes from 0 to 60s. In Fig. 4c, the DNA transfection efficiency exhibits an increasing trend when PRF increases from 0 to 250 Hz, then holds a high level greater than 40% when PRF >250 Hz. It also shows that the cell viability decreases quickly with the increasing of PRF.

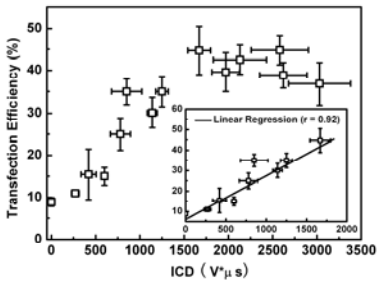

Figure 5. The relationship between the DNA transfection efficiency and ICD, for the pooled data analysis.

As shown in Fig. 3, the influences of the US parameters (*e.g.*, $\bar{P}$, treatment time, or PRF) on ICD show similar trends as those on the DNA transfection efficiency. Thus, with analyzing the pooled data, the relationship between the measured ICD and DNA transfection efficiency can be illustrated in Fig. 5. The enlarged-scale inset in Fig. 5 shows that the DNA transfection efficiency is initially increases linearly with the increasing ICD, then it tends to saturate while the ICD reaches a certain level (*e.g.*, ICD > 1670 V×μs). This phenomenon will be discussed in detail later. Different from the studies regarding the DNA transfection efficiency, linear correlation can be observed between cell viability decreasing and the ICD enhancement (see Fig. 6).

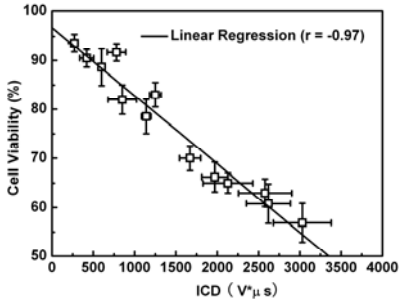

Figure 6. Linear correlation between the cell viability and ICD for the pooled data analysis (r=-0.97).

The correlation between ICD and the generation of sonoporation pore on the cell membranes

In order to better understand the mechanism of US-mediated sonoporation, the influence of ICD on the generation of sonoporation pore were systemically investigated with varied US parameters, based on SEMs. The tested US conditions were divided into three series as introduced in previous sections.

An intact MCF-7 cell should have a spherical shape and a relative smooth surface. Fig.7 shows the membrane morphology of MCF-7 cells exposed to US pulses with varied varied $\bar{P}$, treatment time, and PRF, respectively (in Fig.7a, b, and c). It is obvious that, when cells were sonicated at low US energy (*e.g.*, P =0.3 MPa; treatment time=5 s; or PRF=20 Hz), some tiny "holes" appeared on the cell membranes. With the increasing of US parameters (higher P , longer treatment time, or faster PRF), larger sonoporation pores and more rough regions were observed on the cell membranes, while the cell still kept its general morphology. When the US parameters got to a certain high lever (*e.g.*, P =3.0 MPa; 60-s treatment time; or 1000-Hz PRF), the sonoporation pore size enlarged conspicuously and the cell surface buckled severely, which might cause unrecoverable damage to the cell.

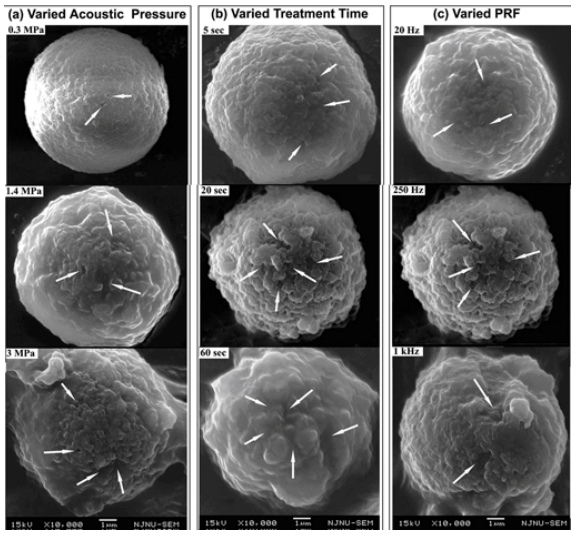

Figure 7. Morphology of cells exposed to 20-cycle US pulses at 1 MHz, with varied (a), acoustic pressure ($\bar{P}$), (b) US treatment time, and (c) PRF. The white arrows point out some sonoporation pores.

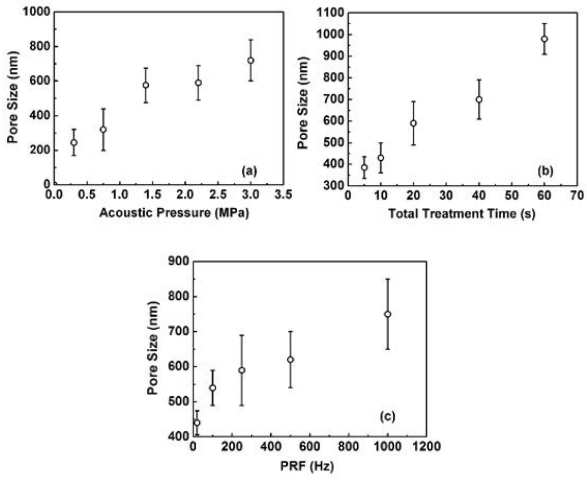

Figure 8. The influences of US parameters on sonoporation pore size. (a) the sonoporation pore sizes measured according to SEM images are plotted as a function of $\bar{P}$, with PRF=250 Hz, treatment time=20 s; (b) pore size *vs.* treatment time, with $\bar{P}$ = 2.2 MPa, PRF=250 Hz; (c) the relationship between pore size and PRF, with $\bar{P}$ = 2.2 MPa, treatment time=20 s.

All the SEM images were read as gray-scale intensity figures using MATLAB software, and the sizes of sonoporation pores were estimated according to the scale marked on the SEM image. Five replicate experiments were carried out for every tested US conditions, and 10 cells were selected for SEM investigation in each sonicated sample. As shown in Fig.8, the pore size ranges from ~150 nm to 1 μm. It can be noticed that the sonoporation pore size increases with the increasing of P , treatment time and PRF. Based on the further investigation of the pooled data, high correlation could

be observed between the sonoporation pore size and the measured ICD (Fig. 9). It also shows in Fig. 10 that the cell viability is linearly decreases with the increasing of pore size.

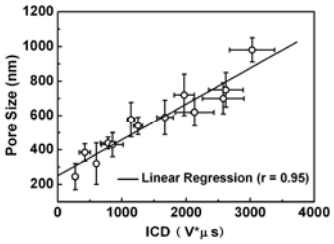

Figure 9. Linear correlation between ICD and sonoporation pore size (r = 0.95).

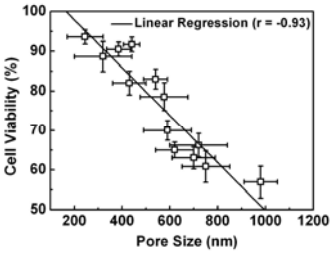

Figure 10. Linear correlation of sonoporation pore size and cell viability (r = -0.93).

DISCUSSION

Current studies systemically examined the relationship between the IC activities and US-mediated DNA transfection. MCF-7 cells mixed with PEI: DNA complexes and UCA microbubbles were exposed to 1-MHz US pulses with varied acoustic parameters (*e.g.*, P^-, total treatment time, PRF). The "amount" of effective IC activities generated during the US exposure were detected with PCD system and evaluated as ICD. The US-mediated DNA transfection efficiency and cell viability were investigated based on flow cytometry assessment. Meanwhile, the sonoporation effect on the cell membrane was examined using SEM. All the specific hypotheses were supported well with repeatable experimental results.

PEI：DNA complexes were used in this work instead of naked DNA. It is because that PEI has been shown to be a relatively efficient non-viral vector and been used successfully for *in vivo applications*, including direct application to various anatomical sites [8,29]. Especially, Deshpande and Mrausinitz have reported that the combination of US and PEI can synergistically enhance the DNA transfection [10]. Actually, as shown in Fig. 11, we also verified their conclusion. The DNA transfection efficiencies are 0.9±0.2%, 4±0.5%, 8.9±1%, 10.8+0.8%, and 44.7±5.8%, for cells with (1) naked DNA, no US, (2) naked DNA and UCA, exposed to US, (3) PEI:DNA, no US, (4) PEI:DNA, exposed to US, and (5) PEI:DNA and UCA, exposed to US, respectively. Therefore, it has more practical significance to utilize PEI:DNA complexes in current work instead of naked DNA.

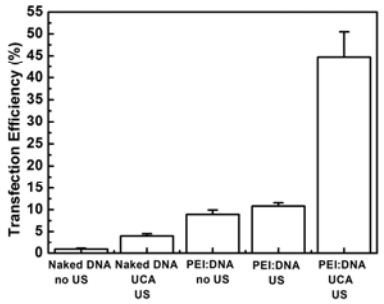

Figure 11. Assessment of DNA transfection efficiency for the cells with (1) naked DNA, no US, (2) naked DNA and UCA, exposed to US, (3) PEI:DNA, no US, (4) PEI:DNA, exposed to US, and (5) PEI:DNA and UCA, with US. At P^- =2.2 MPa, 250-Hz PRF, and 20-s treatment time.

According to the flow cytometry assessments on the GFP expression of cell suspensions sonicated with the presence of PEI:DNA complexes and UCAs, up to 44.7±5.8% DNA transfection efficiency could be obtained under selected US conditions. Previous studies have shown that the DNA transfection efficiency increases with the increasing acoustic pressure and exposure time [7, 10], our results support these conclusions (see Fig. 4a and b). Furthermore, similar increasing trend is also observed with PRF increasing (Fig. 4c). In other words, the DNA transfection efficiency could be affected by the synthetic effect of several US conditions so that it is difficult to simply determine the optimized US parameters. One important hypothesis tested in current work is that it is possible to define a more reasonable indicative term (*e.g.*, ICD) that is closely related with US-mediated DNA transfection effect to help us optimize the US conditions. As pointed in earlier literatures [17, 19], acoustic cavitation should be one of the most important mechanisms of sonoporation and adding UCAs (serve as nuclei) can enhance cavitation activities. As shown in Fig. 11, the DNA transfection efficiency measured for the samples sonicated without UCAs is only low to 10.8+0.8%, which provides solid proof to the important role of IC activity on the US-mediated DNA transfection. However, no direct quantitative measurement has been reported to assess the cumulative IC effects involved in US-mediated DNA transfection. In this paper, the detected broad-band IC noise signals were quantified as IC dose, which could not only reflect the intensity of IC activity, but also evaluate the "amount" of cavitation effects cumulated over the US exposure duration. As illustrated in Fig. 5, for the pooled data, linear correlation can be observed between the DNA transfection efficiency and ICD within a certain range (*e.g.*, 0< ICD <1670 V×μs), which suggests that ICD might be used as an effective index to monitor and control the IC activities associated with US-mediated gene/drug delivery to achieve the most desired transfection effect, if combined with sufficient statistic studies. Nevertheless, instead of monotonically increased with ICD, the DNA transfection efficiency tends to saturate or even slightly decreased as the ICD reaches a high level (*e.g.*, ICD > 1670 V×μs). This phenomenon could be explained by the significant decrease of cell viability. As shown in Fig. 6, the cell viability linearly decreased with increasing ICD. It suggests that large amount of cells would be killed due to the superabundant acoustic energy supplies, which can impair the DNA transfection outcomes.

Previous reports have suggested that US-mediated DNA transfection should be related to the sonoporation by generating transient pores on the cell membrane [30-32]. In order to further understand the mechanism of IC activities act on the DNA transfection and cell viability, the relationship between

sonoporation outcomes and the measured ICD was explored by examining the sonoporation pores generated on the sonicated cell membranes based on SEM images (see Fig. 7) with varied US parameters. As shown in Fig. 8, the estimated pore size enlarges from 150 nm to 1 μm with US parameter (*viz.*, P^-, treatment time, and PRF) increasing. The normal size of 25kDa PEI:DNA complexes has been reported as ~100-200 nm [33]. Thus, even at the lowest US condition tested here, the sonoporation pores should be wide enough to allow PEI:DNA complexes to enter MCF-7 cells. By analyzing the pooled data, linear correlation can be observed between the sonoporation pore size and ICD (Fig. 9), which provides solid data that the DNA transfection could be facilitated by IC activity through the generation of sonoporation pores. However, we also noticed that the cell viability linearly decreases with the increasing ICD (Fig. 6) and pore size (Fig. 10), which indicates that over-enlarged pores resulting from superabundant IC energy might result in unrecoverable damage to cells, thereby significantly impairing the transfection effect and making the transfection efficiency saturate or even decrease.

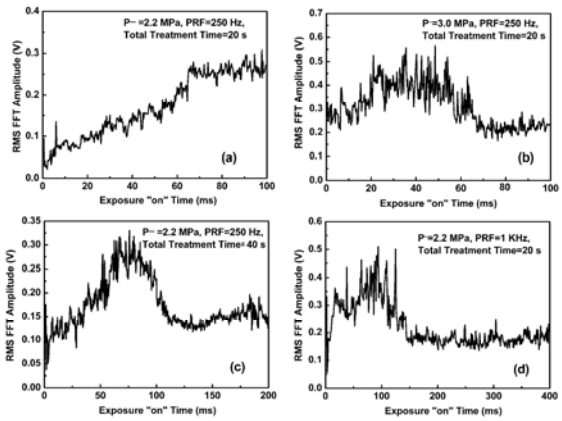

Figure 12. The temporal evolution of the IC intensities (quantified as RMS FFT amplitudes of IC broad-band noise signals within selected frequency window; see details in Sec. 2.2.4) under different US conditions. (a) the cells were exposed to US pulses with P^- = 2.2 MPa, 250-Hz PRF, and 20-s treatment time; (b) the sample was exposed to US pulses with P^- = 3.0 MPa, PRF = 250Hz, and total treatment time = 20s; (c) the sample suspension was exposed to US pulses with P^- = 2.2 MPa, PRF = 250Hz, and total treatment time = 40s; and (d) the sample was exposed to US pulses with P^- = 2.2 MPa, PRF = 1000 Hz, and total treatment time = 20s.

Another interesting point worth to be pointed out here is that the ICD is not linearly increased with the increasing of the delivery US energy (as shown in Fig. 3), and the explanation can be illustrated in Fig. 12, which shows the temporal evolutions of the IC activity intensities generated under different US conditions. For relatively low or moderate US conditions (*e.g.* P^-=2.2 MPa, PRF=250 Hz, and treatment time=20 s), the IC intensity keeps increasing. However, if the US conditions get too high (*e.g.*, P^-=3.0MPa, or treatment time=40s, or PRF=1KHz, the IC intensity will be initialized at a higher level (for example, the initial RMS FFT amplitude of the IC signals at 2.2MPa is lower than 0.1 V, while the corresponding value gotten with 3.0-MPa US exposure is about 0.3 V.), followed by ascending trend within a certain duration, then drops to a base level, which is speculated that most UCA microbubbles should be destroyed quickly by the strong US pulses so that the effective IC activities can not sustained to the end of US exposures and the delivered acoustic energy is mostly wasted. Han *et.al.*[34] had suggested that the UCA concentration or the bubble-to-cell ratio might be another important factor that affected the US-mediated drug delivery. Our current observations support this hypothesis with quantitative analyses. And further study will be focused on the relationship between UCA microbubble concentration and gene/drug delivery effect.

ACKNOWLEDGEMENTS

The authors wish to convey their gratitude for the helpful discussion from Prof. Lawrence A. Crum at University of Washington. This work was funded in part by the National Natural Science Foundations of China (No. 10704037, 10774071, 10974093, 50673041 and 30771036), the National Basic Research Foundation of China (973 2006CB503909 and 2004CB518603), the Research Fund for the Doctoral Program (for new scholar) of Higher Education of China (20070284070).

REFERENCES

1 S. Anderson, Human gene therapy, Science, 256 (1992) 808-813.
2 G. Prasad, H. Wang, D. Hill, R. Zhang, Recent advances in experimental molecular therapeutics for malignant gliomas, Curr. Med. Chem. Anti-cancer Agents, 4 (2004) 347-361.
3 S. Mehier-Humbert, R. Guy, Physical methods for gene transfer: improving the kinetics of gene delivery into cells, Adv. Drug. Deliv. Rev., 57 (2005) 733-753.
4 D. Wilson, Viral-mediated gene transfer for cancer treatment, Curr. Pharm. Biotechnol. 3 (2002) 151-164.
5 T. Niidome, L. Huang, Gene therapy progress and prospects: nonviral vectors. Gene Ther., 9 (2002) 1647-1652.
6 U. Lungwitz, M. Breuning, T. Blunk, Polyethylenimine-based non-viral gene delivery systems, Eur. J. Pharm. Biopharm., 60 (2005) 247-266.
7 M. Neu, D. Fischer, T. Kissel, Recent advances in rational gene transfer vector design based on poly(ethylene imine) and its derivatives, J. Gene Med., 7 (2005) 992-1009.
8 A. Boletta, A. Benigni, J. Lutz, G. Remuzzi, M.R. Soria, L. Monaco, Non-viral gene delivery to the rat kidney with poly(ethylenimine), Hum. Gene Ther., 8 (1997) 1243-1251.
9 A. Kicheler, C. Leborgne, E. Coeytaux, O. Danos, Polyethyleneimine-mediated gene delivery: a mechanistic study. J. Gene Med., 3 (2001) 135-144.
10 M. C. Deshpande, M. R. Prausnitz, Synergistic effects of ultrasound and PEI on DNA transfection in vitro, J. Control. Release, 118 (2007) 126-135.
11 S. Mitragotri, Healing sound: the use of ultrasound in drug delivery and other therapeutic applications, Nat. Rev. Drug Discov., 4 (2005) 255-260.
12 K. Ferrara, R. Pollard, M. Borden, Ultrasound microbubble contrast agents: fundermental and application to gene and drug delivery, Annu. Rev. Biomed. Eng. 9 (2007) 415-447.
13 G. Tsivgoulis, A. V. Alexandrov, Ultrasound-enhanced thrombolysis in acute ischemic stroke: potential, failures, and safety, Neurotherapeutics, 4 (2007) 420-427.
14 I. Rosenthal, J. Z. Sostaric, P. Riesz, Sonodynamic therapy-a review of the synergistic effects of drugs and ultrasound, Ultra. Sonochem., 11 (2004) 349-363.
15 M. Sophie, B. Thierry, Y. Feng, R. Guy, Plasma membrane poration induced by ultrasound exposure implication for drug delivery. J. Control. Release, 104 (2005) 213-222.
16 A. Van Wamel, K. Kooiman, M. Harteveld, M. Emmer, F. J. ten Cate, M. Versluis, N. de Jong, vibrating microbubbles poling individual cells: drug transfer into cells via sonoporation, J. Control. Release, 112 (2006) 149-155.

17 J. Wu, P. Jason, R. Mercedes, Sonoporation, anti-cancer drug and antibody delivery using ultrasound, Ultrasonics, 44 (2006) e21-e25.
18 C. Newman, T. Bettinger, Gene therapy progress and prospects: ultrasound for gene transfer. Gene ther. 14 (2007) 465-475.
19 D. Miller, S. Pislaru, J. Greenleaf, Sonoporation: mechanical DNA delivery by ultrasonic cavitation, Cell Mol. Genet., 27 (2002) 115-134.
20 R. Apfel, C. Holland, Gauging the likelihood of cavitation from short-pulse, low-duty cycle diagnostic ultrasound, Ultra. Med. Biol, 17(2) (1991) 179-185.
21 C. Deng, Q. Xu, R. Apfel, C. Holland, In vitro measurements of inertial cavitation thresholds in human blood, Ultra. Med. Biol., 22 (1996) 939-948.
22 P. Chang, W. Chen, P. Mourad, S. Poliachik, L. Crum, Thresholds for inertial cavitation in Albunex suspesions under pulsed ultrasound conditions, IEEE Trans. Ultra. Ferro. Freq. control, 48 (2001) 161-170.
23 J. Tu, T. Matula, A. Brayman, L. Crum, Inertial Cavitation Dose Produced in Ex Vivo Rabbit Ear Arteries by 1-MHz insonation treatment during infusion with Optison, Ultra. Med. Biol., 32 (2006) 281-288.
24 C. Leborgne, E. Coeytaux, O. Danos, Polyethyleneimine-mediated gene delivery: a mechanistic study, J. Gene Med., 3 (2001) 135-144.
25 E. Cramer, W. Lauterborn, Acoustic cavitation noise spectra, Appl. Sci. Res., 38 (1982) 209-214.
26 E. Everbach, I. Makin, M. Azadniv, R. Meltzer, Correlation of ultrasound-induced hemolysis with cavitation detector output in vitro, Ultra. Med. Biol., 23 (1997) 619-624.
27 N. Kudo, K. Okada, K. Yamamoto, Sonoporation by single-shot pulsed ultrasound with microbubbles adjacent to cells, Biophys. J., 96 (2009) 4866-4876.
28 V. Zamitsyn, C. Rostad, M. Prausnitz, Modeling transmembrane transport through cell membrane wounds created by acoustic cavitation, Biophys. J., 95 (2008) 4124-4138.
29 G. Lemkine, D. Goula, N. Becher, L. Paleari, G. Levi, G. Demeneix, Optimisation of oplyethylenimine based gene delivery to mouse braine, J. Drug Target, 7(1999), 305-312.
30 H. R. Guzman, D. X. Nguyen, S. Khan, M. R. Prausnitz, Ultrasound-mediated distruption of cell membranes. I. Quantification of molecular uptake and cell viability, J. Acoust. Soc. Am., 110 (2001) 588-596.
31 P. Schelicher, H. Radhakrishna, T. Tolentino, R. Apkarian, V. Zamitsyn, M. Prausnitz, Mechanism of intracellular delivery by acoustic cavitation, Ultra. Med. Biol., 32 (2006) 915-924.
32 F. Yang, N. Gu, D. Chen, X. Xi, D. Zhang, Y. Li, Junru Wu, Experimental study on cell self-sealing during sonoporation, J. Control. Release, 131 (2008) 205-210.
33 P. Erbacher, T. Bettinger, P. Belguise-Valladier, S. Zou, J. Coll, J. Behr, J. Remy, Transfection and physical properties of various saccharide, poly (ethylene glycol), and antibody-derivatized polyethylenimines (PEI), J. Gene Med., 1 (1999) 210-222.
34 Y. Han, A. Ikegami, P. Chung, L. Zhang, C. Deng, Sonoporation is an efficient tool for intracellular fluorescent dextran delivery and one-step double-crossover mutant construction in Fusobacterium nucleatum, Appl. Environ. Microbiol. 73 (2007) 3677-3683.